Dilute gas viscosity of *n*-alkanes represented by rigid Lennard-Jones chains

Juan Carlos Castro-Palacio,† Robert Hellmann,‡ and Velisa Vesovic†,[a]

† Department of Earth Science and Engineering, Imperial College London, London SW7 2AZ, United Kingdom.

‡ Institut für Chemie, Universität Rostock, 18059 Rostock, Germany.

a) Author to whom correspondence should be addressed. Electronic mail: v.vesovic@imperial.ac.uk.

Abstract

The shear viscosity in the dilute gas limit has been calculated by means of the classical trajectory method for a gas consisting of chain-like molecules. The molecules were modelled as rigid chains made up of spherical segments that interact through a combination of site-site Lennard-Jones 12-6 potentials. Results are reported for chains consisting of 2, 3, 4, 6, 8, 12 and 16 segments in the reduced temperature range of 0.3 – 50 for site-site separations of 0.25σ, 0.333σ, 0.40σ, 0.60σ and 0.80σ, where σ is the Lennard-Jones length scaling parameter. The results were used to determine the shear viscosity of *n*-alkanes in the zero-density limit by representing an *n*-alkane molecule as a rigid linear chain consisting of $n_c - 1$ spherical segments, where n_c is the number of carbon atoms. We show that for a given *n*-alkane molecule, the scaling parameters ε and σ are not unique and not transferable from one molecule to another. The commonly used site-site Lennard-Jones 12-6 potential in combination with a rigid-chain molecular representation can only accurately mimic the viscosity if the scaling parameters are fitted. If the scaling parameters are estimated from the scaling parameters of other *n*-alkanes, the predicted viscosity values have an unacceptably high uncertainty.

Keywords: *n*-alkanes, viscosity, dilute gas, Lennard-Jones chains

1. Introduction

The viscosity of a dilute gas can be related, by means of kinetic theory, to the binary molecular collisions, which are governed by intermolecular forces [1]. For dilute gases consisting of simple molecules, it is possible to calculate the viscosity directly from *ab initio* intermolecular potential energy surfaces. The calculations have been performed for a number of molecular systems such as diatoms [2,3], linear triatoms [4], spherical tops [5], polar asymmetric tops [6,7] and, most recently, mixtures [8,9]. The molecular collisions were computed by means of classical trajectories, treating molecules as rigid rotors, while the full kinetic theory of polyatomic gases [1] has been used to calculate the viscosity. The accuracy of the calculated viscosity values is generally commensurate with the best available experimental data, and all the recent studies [2-9] demonstrate that the viscosity in a dilute gas limit can be calculated to better than 0.5-1.0%.

For larger molecules, such calculations are still not feasible as the inclusion of vibrational degrees of freedom into the classical trajectory calculations is not fully resolved and the development of *ab initio* potential surfaces for different vibrational states is prohibitively computationally expensive. To make such calculations feasible, one resorts to model systems where the intermolecular forces are represented by simple potentials and the molecules are treated as rigid rotors. In a recent classical trajectory calculation [10], the molecules were modelled as rigid chains consisting of spherical segments that interact through a combination of site-site Lennard-Jones (LJ) 12-6 potentials. The viscosity in the dilute gas limit for a gas consisting of such chain-like molecules increases with temperature and decreases with chain length, thus mimicking the behavior observed in real gases.

In this work, we extend our previous study [10] on the viscosity of a gas consisting of chain-like molecules to the calculation of the viscosity of normal, paraffinic alkanes (*n*-alkanes) in the dilute gas limit. The *n*-alkanes are an industrially important chemical family with widespread use and, at least for smaller *n*-alkanes, there is plentiful, reliable gas viscosity data at low pressures. As the number of carbon atoms increases, *n*-alkanes structurally resemble long chains made up of ($-CH_2$) units and thus are ideal to test the usefulness of models consisting of chain-like molecules interacting through site-site intermolecular potentials. In this paper, we are primarily interested in testing three hypotheses: (i) Is the site-site LJ 12-6 potential sufficiently realistic to represent the viscosity of *n*-alkanes in the dilute gas limit; (ii) are the energy and length scaling parameters of the LJ 12-6 potential transferrable from one *n*-alkane molecule to another; (iii) if they are not, is there a trend among *n*-alkane LJ 12-6 scaling parameters that will allow for the prediction of the viscosity of an *n*-alkane for which there is a lack of experimental viscosity data.

The choice of the LJ 12-6 potential was driven primarily by its simplicity and its popularity in molecular dynamics (MD) simulations. The developments in MD have allowed for the calculation of viscosity to be

performed over most of the phase space. Galliéro and co-workers have carried out molecular dynamics simulations of ideal fluids [11-15] using LJ 12-6 potentials and subsequently developed correlations for the estimation of the viscosity of real fluids [11,12]. Patra and co-workers [16] have reported results for two- and three-dimensional LJ chains of varying lengths and have examined how the dimensionality affects the viscosity of dense fluids. Goel *et al.* [17] have used the LJ chains concept to investigate viscosity scaling based on excess entropy, while Zhang and Yu [18] have extended this further and proposed a viscosity equation for fluids modelled as freely jointed LJ chains. Vrabec and collaborators [19,20] have used site-site LJ potentials to correlate the thermophysical properties, including viscosity, of cyclic alkanes and small molecules. Numerous authors have used the effective spherical LJ 12-6 potential to investigate the viscosity of real and ideal fluids by means of molecular simulations [21-28]. The preponderance of the LJ 12-6 potential in MD simulations gives the current work a more general context of testing its limitations, albeit only in the dilute gas limit, where a combination of the kinetic theory and classical trajectory calculations provide us with an accurate method of calculating the viscosity.

The recent work [29] on using the effective spherical LJ 12-6 potential to calculate the viscosity of small alkanes by means of kinetic theory has indicated that the agreement with experimentally measured viscosity values is remarkably good, within 1–2%. This was achieved by constraining the LJ length scaling parameter, σ, and optimizing the energy scaling parameter, ε, for each alkane. The resulting energy scaling parameters exhibit a monotonic increase as a function of carbon number, which was used to develop a simple correlation that allows viscosity prediction for *n*-alkanes for which no measurements are available. The site-site LJ 12-6 potential offers a more realistic representation of the anisotropic intermolecular potential than a simple effective spherical potential. It also allows for the full use of the kinetic theory of polyatomic gases, thus allowing for rotational-translational energy transfer. However, it assumes that *n*-alkane molecules can be represented as rigid chains, thus not taking into account any bending or folding of *n*-alkane chains. There is strong evidence from molecular simulations [11-15] that the lack of flexibility impacts on the viscosity of longer chains, at least in the dense fluid. Nevertheless, the site-site LJ 12-6 potential is an effective one in the same way as is the previously discussed spherical LJ 12-6 potential [29]. So, the questions are: (i) can the choice of the length and energy scaling parameters for the site-site potentials be made such as to compensate for the deficiencies of the current model and (ii) will this produce a more accurate way of calculating the viscosity than was achieved by means of an effective spherical LJ 12-6 potential.

The outline of this article is as follows. In Section 2, we describe the representation of the *n*-alkanes by rigid linear chains and the choice of experimental viscosity data. In Section 3, the sensitivity of the viscosity to the site-site distance is discussed, the results of the fitting procedure used to obtain the optimal LJ scaling

parameters are presented and the calculated viscosity values are compared with experimental data for each *n*-alkane. Summary and conclusions are given in Section 4.

2. Methodology

In line with our previous work [10], we examine collisions of two rigid linear chains that interact through a combination of site-site intermolecular forces. Each chain is made up of n_s linearly arranged spherical segments, each of mass m_s with a site placed at the center of each segment. The site-site interaction is modelled by a simple LJ 12-6 potential, characterized by the parameter σ, which defines the characteristic length at which the intermolecular potential is zero, and the parameter ε, which defines the characteristic energy that represents the well depth of each site-site interaction. In the present calculations, the distance between two neighbouring sites, s, is allowed to vary and is no longer made equal to the LJ parameter σ [10].

The shear viscosity in the zero-density limit, η, of a gas consisting of such rigid chains can be expressed by the traditional kinetic theory result as [1]

$$\eta = \frac{k_B T}{\langle v \rangle_0} \frac{f_\eta^{(n)}}{\Im(2000)} \quad , \tag{1}$$

where $\langle v \rangle_0 = 4(k_B T/\pi m)^{1/2}$ is the average relative thermal speed, k_B is the Boltzmann's constant, T is the temperature, m is the mass of the chain and $\Im(2000)$ is a generalised cross section. The generalised cross sections include all of the information about the dynamics of the binary collisions that govern transport properties and the notation and conventions employed are fully described elsewhere [1-10]. Here, for simplicity we have used the symbol η to indicate the viscosity in the zero-density limit, rather than the more traditional η_0 [30]. The quantities $f_\eta^{(n)}$ are the n^{th} order correction factors, which can be expressed in terms of generalised cross sections [4,5,31]. In this work, we have calculated the viscosity up to the third-order correction factor in line with most of our previous work [5,7-9]. The generalised cross sections were computed by means of the classical trajectory method using a modified version of the TRAJECT software code [32], the details of which are given in our previous work [10].

In this work, we are primarily interested in the influence of changing the site-site distance, s, and the resulting intermolecular potential anisotropy on the viscosity and on representing the viscosity of *n*-alkane molecules by the described chain model. Hence, it is more convenient [10] to work in terms of reduced rather than absolute quantities. We make use of the definition of the reduced viscosity that has already been used by a number of investigators [10,12],

$$\eta(T;s) = \eta^*(T^*;s^*)\, m_s^{1/2}\, k \ , \tag{2}$$

$$T^* = T/\varepsilon \ , \tag{3}$$

$$s^* = s/\sigma \ , \tag{4}$$

where $k \equiv \sqrt{\varepsilon}/\sigma^2$ and the reduced quantities are denoted by an asterisk. We note that we have used the LJ potential parameters ε and σ as the characteristic energy and length, respectively, to define the reduced quantities. We have evaluated the reduced viscosity as a function of the reduced temperature ($T^* = 0.3 - 50$) for different chains characterized by the number of segments, $n_s = 2, 3, 4, 6, 8, 12, 16$ and by different values of the reduced site-site distance, $s^* = 0.25, 0.333, 0.40, 0.60, 0.80$. We have used these results, together with results for $s^* = 1$ from our previous work [10], in the further analysis.

2.1. *Representation of the n-alkanes*

One of the main objectives of this work is to examine if the proposed LJ chain model can be used to successfully represent the viscosity of *n*-alkanes. The most natural representation of an *n*-alkane molecule by a rigid linear-chain model is to use the ball and stick model [33] and place the segment sites in between two neighbouring carbon atoms. This would result in representing an alkane molecule using $n_s = n_c - 1$ segments, where n_c is the number of carbon atoms. Figure 1 shows a schematic representation of *n*-pentane as represented by a linear chain of four segments.

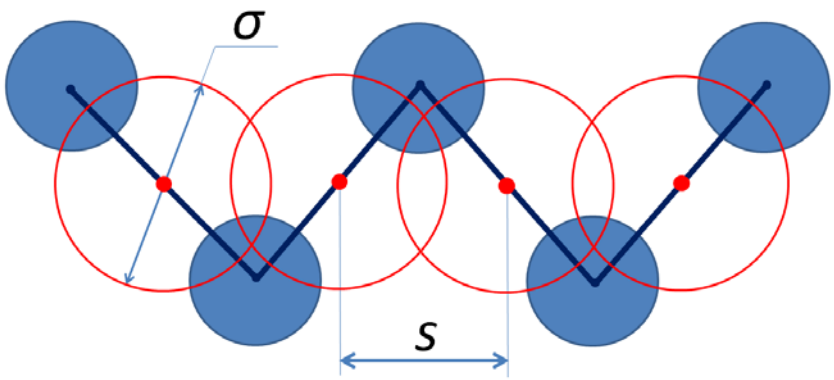

Figure 1: Schematic representation of *n*-pentane by a rigid linear chain of four spherical segments. The blue circles represent the carbon atoms, while the red open circles represent segments.

Bearing in mind that our LJ model assumes that the chains consist of segments of identical mass that interact with the same effective site-site potential (i.e., the same values of ε and σ are used for all site-site interactions between two chains), we have limited our analysis to *n*-alkanes that have the chemical structure CH_3-$(CH_2)_n$-CH_3 ($n \geq 1$). Hence, the shortest *n*-alkane we have examined is propane. To make the model as realistic as possible, we constrain the parameters m_s and s such that the resulting values for the molecular weight (M_w) and moment of inertia (I), of the linear chain about an axis perpendicular to the

molecular axis and passing through the center of mass, are the same as those for the alkane molecule. This ensures that the inertial properties, which strongly influence the exchange of rotational and translational energy during collisions, are properly accounted for. It also provides us with a unique value of the site-site distance, *s*, for each alkane molecule based on the published data on molecular weight [34] and moment of inertia [33]. For instance for propane we obtain a simple expression for the site-site distance, $s = 2\sqrt{I/M_w}$, which can be easily shown to be equal to twice the radius of gyration of the propane molecule. The moment of inertia for *n*-alkanes up to and including *n*-decane was obtained from Ref [33], while for longer *n*-alkanes the moment of inertia was estimated by extrapolating the correlation given in the same reference. Table 1 summarizes the resulting values of s for the alkanes considered in this work, together with a nominal length of each chain defined as $l = sn_s$. For all alkanes, the value of s is smaller than nominal distance between adjacent, unbonded carbon atoms namely, $2d\sin(\alpha/2) = 0.256\ \mathrm{nm}$ (see Figure 1), where $d = 0.1526\ \mathrm{nm}$ is the typical equilibrium C-C bond length [35] and $\alpha = 113.8º$ the typical C-C-C angle [35].

Table 1: Results for the site-site distance, s, and the length of the chain, l, for the *n*-alkanes studied in this work.

***n*-alkane**	$\boldsymbol{s}$ **(nm)**	$\boldsymbol{l}$ **(nm)**
C_3H_8	0.2302	0.4604
C_4H_{10}	0.1853	0.5558
C_5H_{12}	0.1675	0.6700
C_6H_{14}	0.1580	0.7898
C_7H_{16}	0.1520	0.9119
C_8H_{18}	0.1479	1.0356
C_9H_{20}	0.1447	1.1576
$C_{10}H_{22}$	0.1426	1.2838
$C_{12}H_{26}$	0.1410	1.5511
$C_{13}H_{28}$	0.1400	1.6800
$C_{14}H_{30}$	0.1392	1.8090
$C_{16}H_{34}$	0.1378	2.0672

We observe that for small *n*-alkanes the site-site distance rapidly decreases with carbon number before reaching a plateau for larger *n*-alkanes. The length of the chain increases nearly linearly with the number of

carbon atoms in the *n*-alkane molecule. We note that for s^*=1 the expression for the total bond distance defined as $s(n_s-1)$ is the same as the commonly used expression in PC-SAFT.

2.2. *Fitting of the LJ parameters*

In order to rigorously test the proposed model, it is essential to make use of the best available experimental viscosity data, selected on the basis of a critical analysis of the measurement methods. As the viscosity in the zero-density limit is not a quantity directly accessible from experiment, but is obtained by extrapolating the viscosity data measured at low density, it is important to properly take into account the initial density dependence behaviour [36]. This is especially critical for longer alkanes, where for the temperatures of interest ($\sim 250 < T/\mathrm{K} < \sim 700$ K) the vapor pressure is low, limiting the accessibility to measurements, and the contribution of the initial density term cannot be ignored. We have thus performed a critical assessment of the available experimental data and chosen viscosity correlations for four different gases as primary data [37-40]. We have opted to use correlations, as the development of each correlation already involved an extensive analysis of the available experimental data, testing their consistency and providing values over the widest temperature range possible. For brevity, we refer to the viscosity data generated from these correlations as experimental data in the further discussion. Table 2 summarizes the four correlations, detailing the temperature range and the authors' claimed uncertainty.

Table 2: Experimental viscosity data used in this work.

***n*-alkane**	**Authors**	**Temperature range, ΔT_i (K)**	**Claimed uncertainty (%)**
C_3H_8	Vogel *et al.* [37]	293–625	<0.4
C_4H_{10}	Vogel *et al.* [38]	293–600	<0.4
C_6H_{14}	Michailidou *et al.* [39]	298–638	<0.3
C_7H_{16}	Michailidou *et al.* [40]	317–633	<0.3

The LJ parameters, ε and σ, that allow for the best fit of the experimental data have been obtained by minimizing the following objective function,

$$\Delta = \max \left| \frac{\eta_{\mathrm{LJ}} - \eta_{\mathrm{exp}}}{\eta_{\mathrm{exp}}} \right|_{\Delta T_i} , \qquad (5)$$

where η_{LJ} and η_{exp} are the calculated and the experimental viscosity, respectively. This function represents the maximum value of the absolute relative deviation over the experimental range of temperature (ΔT_i) for each *n*-alkane. In order to minimize Δ, we have used a code that evaluates η_{LJ} for a range of the LJ parameters ε and σ (see Equation (2)). The initial ε - σ parameter space, to be discussed later, was chosen such that the reduced quantities s^* and T^* remain within the calculated range ($0.25 \leq s^* \leq 1.0$ and $0.3 \leq T^* \leq 50$) during the minimization procedure. Thus, the η^* data obtained by the classical trajectory method only had to be interpolated, not extrapolated.

3. Results and Discussions

3.1. Sensitivity to site-site distance s

Figure 2 shows the calculated reduced viscosity η^* for a reduced site-site distance of $s^* = 0.25$ as a function of the reduced temperature T^* and as a function of the number of segments n_s. The reduced viscosity exhibits a qualitatively similar behavior to that previously reported [10] for $s^* = 1$.

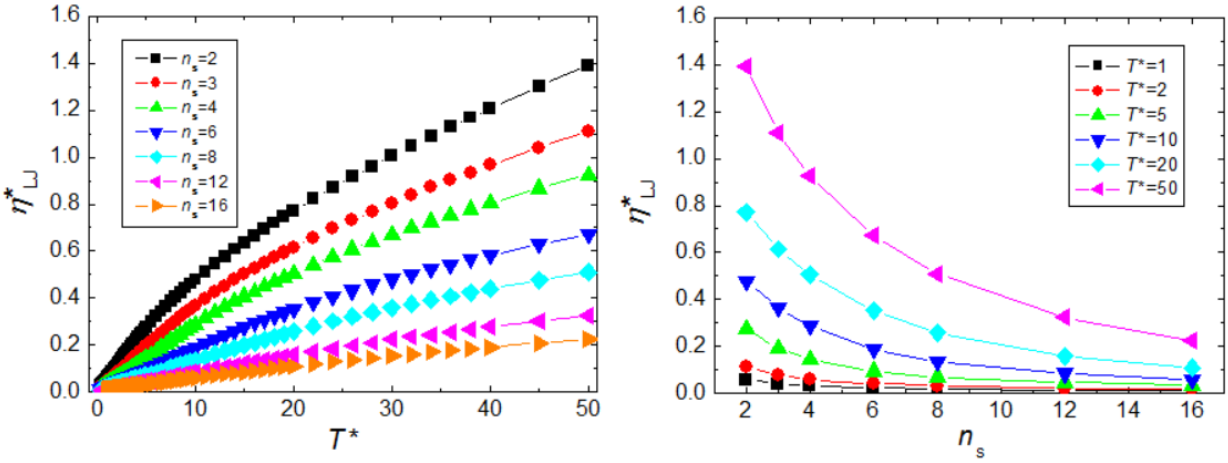

Figure 2: Reduced viscosity, η^*_{LJ}, of rigid LJ chains for $s^* = 0.25$ as a function of the reduced temperature T^* (left panel) and the number of segments per chain n_s (right panel).

Figure 3 shows the behavior of the reduced viscosity as a function of the reduced site-site distance s^* for a number of selected reduced temperatures T^*. We predominantly observe an increase in reduced viscosity with decreasing s^* for a given number of segment n_s. For a chain of a fixed number of segments, the reduction in site-site separation makes the overall chain shorter, resulting in a decrease of the anisotropy of the potential, but primarily in making the effective size smaller, which leads to a smaller cross section $\Im(2000)$ and therefore to a higher viscosity, see Equation (1). As Figure 3 illustrates, the increase in viscosity with reduction of the site-site separation s^* is more pronounced at higher reduced temperatures. In our previous work [10], we established that at $T^* > 5$ the viscosity of the chain is determined by an effective repulsive potential ($V \propto r^{-\alpha}$). The hardness of that effective potential, measured by the parameter α, increases with chain length, varying for example from $\alpha = 19.3$ to $\alpha = 33.4$ when going from the trimer to the hexadecamer [10]. A reduction in s^* shortens the chain and should have a similar effect as a reduction of the number of segments. We would therefore expect a similar decrease in the parameter α. As the viscosity, at least in the first-order approximation, exhibits a $T^{(1/2+2/\alpha)}$ temperature dependence [10,41], it can be easily seen that for a fixed number of segments the ratio of the reduced viscosity at $s^* = 0.25$ (with the corresponding value of α denoted as $\alpha_{0.25}$) to that at say $s^* = 1.0$ has the temperature

dependence $T^{(2/\alpha_{0.25}-2/\alpha_{1.0})}$. Thus, at higher temperatures the increase in reduced viscosity for the same change in s^* will be larger since $\alpha_{1.0} > \alpha_{0.25}$.

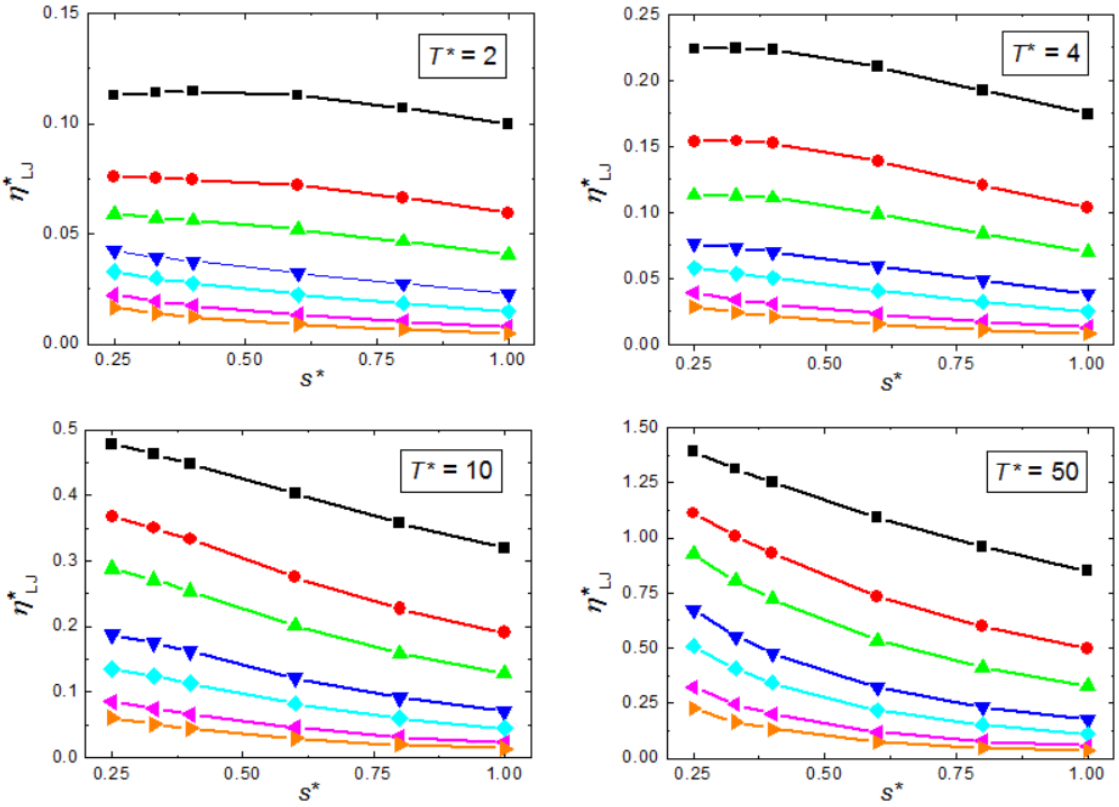

Figure 3: Reduced viscosity, η^*_{LJ}, as a function of reduced site-site distance, s^*, for $T^* = 2,\ 4, 10$ and 50. The different curves represent the different number of segments: (—■—), $n_s = 2$; (—●—), $n_s = 3$; (—▲—), $n_s = 4$; (—▼—), $n_s = 6$; (—◆—), $n_s = 8$; (—◀—), $n_s = 12$; (—▶—), $n_s = 16$.

The contribution of the higher-order correction factor $f_\eta^{(n)}$ to the shear viscosity was analyzed in previous work [10]. It was demonstrated that $f_\eta^{(2)}$ increases rapidly with temperature for low temperatures before beginning to level off in the region $5 < T^* < 10$. The magnitude of the correction increases with chain length, which is a direct result of the increase in the non-sphericity of the potential. Figure 4 illustrates the second-order viscosity correction factors $f_\eta^{(2)}$ for four different reduced site-site separations. For $s^* = 0.60$, we observe a very similar qualitative behavior to what we have reported previously for $s^* = 1.0$ [10], although the saturated values are marginally smaller. For the hexadecamer, the second-order correction factor reaches a value of approximately 1.026 and 1.033 at the highest temperature for $s^* = 0.60$ and $s^* = 1.0$, respectively. The increase in $f_\eta^{(2)}$ is a result of the increase in anisotropy of the potential as discussed before. The reduction of the site-site separation to $s^* = 0.25$ changes the picture; we observe that chains containing more than six segments do not exhibit a saturation value in the investigated temperature range up to $T^* = 50$, and the positions of the minima in $f_\eta^{(2)}$ shift to higher T^* values.

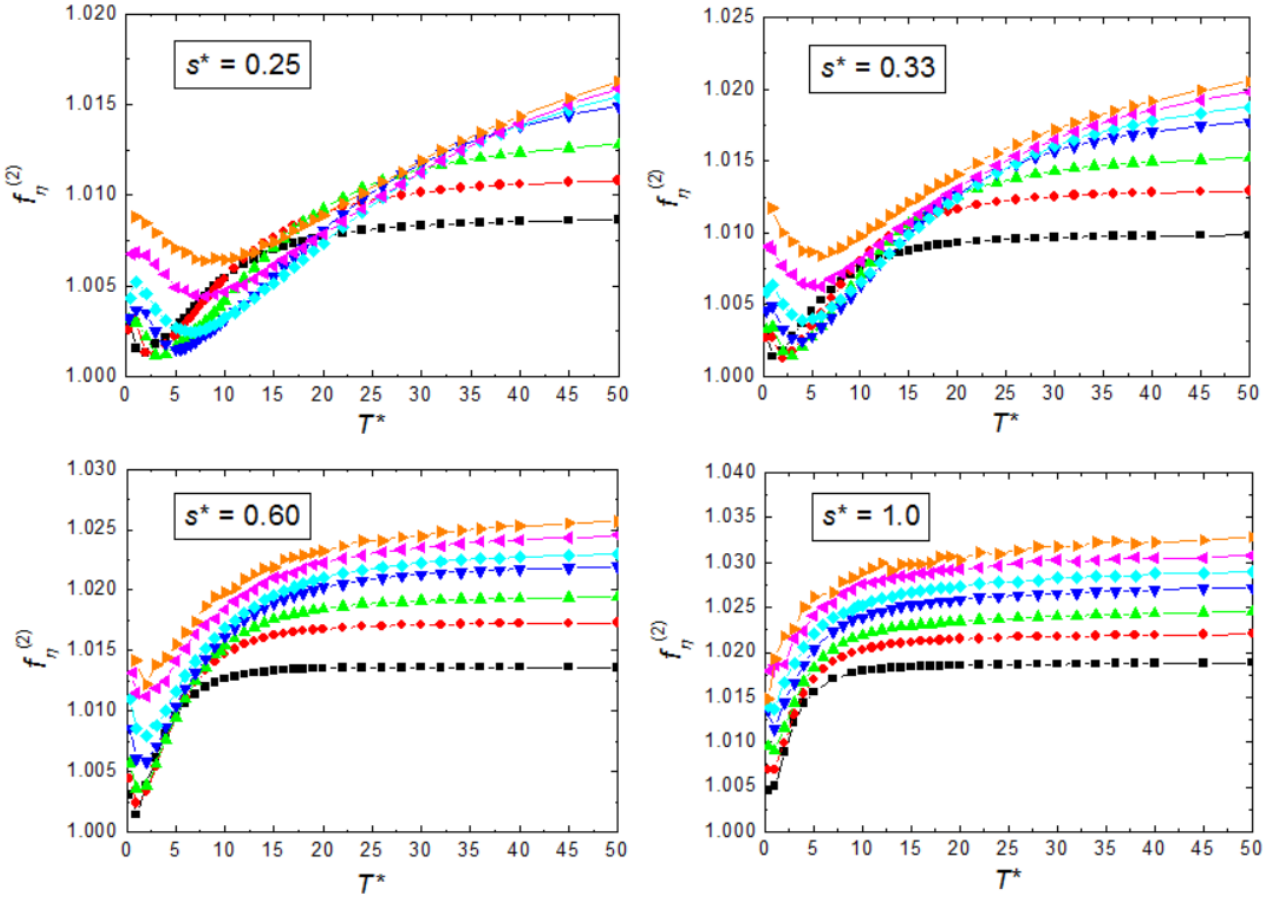

Figure 4: Second-order viscosity correction factor $f_\eta^{(2)}$ of rigid Lennard-Jones chains as a function of the reduced temperature T^* for $s^* = 0.25, 0.333, 0.60$ and 1.0. The different curves represent the different number of segments: (—■—), $n_s = 2$; (—●—), $n_s = 3$; (—▲—), $n_s = 4$; (—▼—), $n_s = 6$; (—◆—), $n_s = 8$; (—◀—), $n_s = 12$; (—▶—), $n_s = 16$.

3.2. *Comparison to experimentally correlated viscosity*

As discussed in the Introduction, one of the objectives of this work was to investigate if there exists a global LJ parameter set (ε and σ) that will allow for an accurate calculation of the viscosity of the whole series of *n*-alkanes by the proposed linear, rigid chain model. If the pathology of the model prevents such an application, the second objective was to determine a LJ parameter set for each alkane and explore if there is a trend that will allow for the prediction of the viscosity of *n*-alkanes for which there is a lack of experimental viscosity data. We start the analysis by determining the optimal LJ parameter sets for four *n*-alkanes (propane, *n*-butane, *n*-hexane and *n*-heptane), for which reliable sets of data are available as illustrated in Table 2.

For each of the four alkanes, the viscosity, η_{LJ}, was calculated using the reduced viscosity obtained from the classical trajectory calculations by choosing the values of the LJ parameters in the overall range $20 \leq \varepsilon/\mathrm{K} \leq 500$ and $0.30 \leq \sigma/\mathrm{nm} \leq 0.50$. Restricting the values to this range avoided the need to extrapolate outside the set of the calculated reduced viscosity data and ensured that the optimum values of the LJ parameters fall within the generally accepted range [42]. As the classical trajectory calculations were performed at only five values of s^*, a reproducing kernel Hilbert space (RKHS) interpolation [43] was used to calculate the reduced viscosity at s^* values determined for each alkane. This interpolation procedure has been successfully used in classical molecular dynamics studies [44,45].

The increments for the parameters used in the gridding were $\Delta\varepsilon = 1\ \mathrm{K}$ and $\Delta\sigma = 10^{-4}\ \mathrm{nm}$. In order to check that our gridding scheme is appropriate, a second grid using a smaller increment for ε ($\Delta\varepsilon = 0.1\ \mathrm{K}$) was computed. The overall minimum values of the objective function Δ (see Equation (5)) are: 0.45%, 0.61%, 0.98% and 1.61% for C_3H_8, C_4H_{10}, C_6H_{14} and C_7H_{16}, respectively. The values for the second grid are very similar, to within 0.01%, which indicates that extra accuracy is not gained by making the grid any finer. Figure 5 shows the relative deviations between the calculated values and the experimental viscosity data.

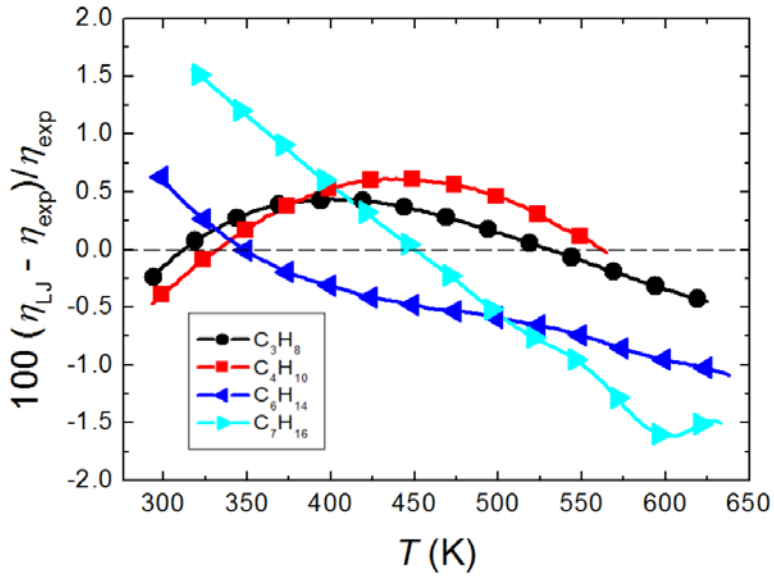

Figure 5: Relative deviations between the calculated viscosity, η_{LJ}, and the experimental viscosity, η_{exp}. The solid lines represent the RKHS interpolation.

We observe that for propane and *n*-butane the experimental data are reproduced with a maximum deviation of 0.45% and 0.6%, respectively, which is just outside their claimed uncertainty of 0.4%. For *n*-hexane and *n*-heptane, the deviations are larger, with the maximum deviations reaching 1.6% and 1.1%, respectively, and we observe a systematic temperature trend for *n*-heptane. It is interesting to note that using an effective spherical LJ 12-6 potential, reported in our previous work [29], the same experimental

data are reproduced with a similar accuracy; the maximum deviations for propane, *n*-butane, *n*-hexane and *n*-heptane are 0.7%, 1.1%, 1.2% and 1.7%, respectively.

Figures 6 and 7 illustrate contours of the maximum average deviation of the calculated viscosity values from the experimental ones, in the energy – length (ε - σ) parameter space representation, for propane and *n*-butane. The results indicate that there is no unique LJ parameter pair. Instead, values of ε and σ can be chosen along the band such that the deviations still remain within a given range (e.g. 1%). A similar non-uniqueness was observed when using spherical LJ potentials to calculate viscosity [29,41] and also in recent work on using the SAFT-VR equation of state to describe thermodynamic properties of water [46]. In the case of viscosity, the non-uniqueness of ε and σ can be attributed to the temperature range of the available data [47]. The larger the reduced temperature range, the smaller the set of LJ parameters that would reproduce the viscosity data within a certain relative deviation. It is also clear that for propane and *n*-butane there is no single set of ε and σ that will reproduce the viscosity of both gases with acceptable accuracy. Figure 7 illustrates the same type of contour plot, but with all four alkanes superimposed. Although the bands for *n*-hexane and *n*-heptane are nearer to each other than are the bands for propane and *n*-butane, the observed bands neither cross nor overlap. This clearly shows that it is not possible to find a unique pair of LJ parameters to represent the viscosity of the four selected *n*-alkanes. It indicates that a global LJ site-site potential is not sufficiently flexible to be transferable from one *n*-alkane molecule to another, in order to characterize their effective interaction relevant to the viscosity. In other words, the change in the potential when increasing the number of segments in the chain does not mimic the change in the potential when going from one *n*-alkane molecule to another. It is possible that a more flexible site-site potential can better address the change in anisotropy of real *n*-alkanes. The Mie n-6 potential is a likely candidate as it enhances the flexibility of the LJ potential by incorporating a parameter that determines the steepness of the repulsive wall [48]. Although it proved successful in describing transport properties at high temperatures [10] and thermodynamic properties by means of the SAFT-γ Mie EOS [49-51], it has been used in most studies as an effective spherical potential. Only recently there have been some molecular dynamics simulations of thermodynamic properties reported based on the site-site Mie potential [52-53].

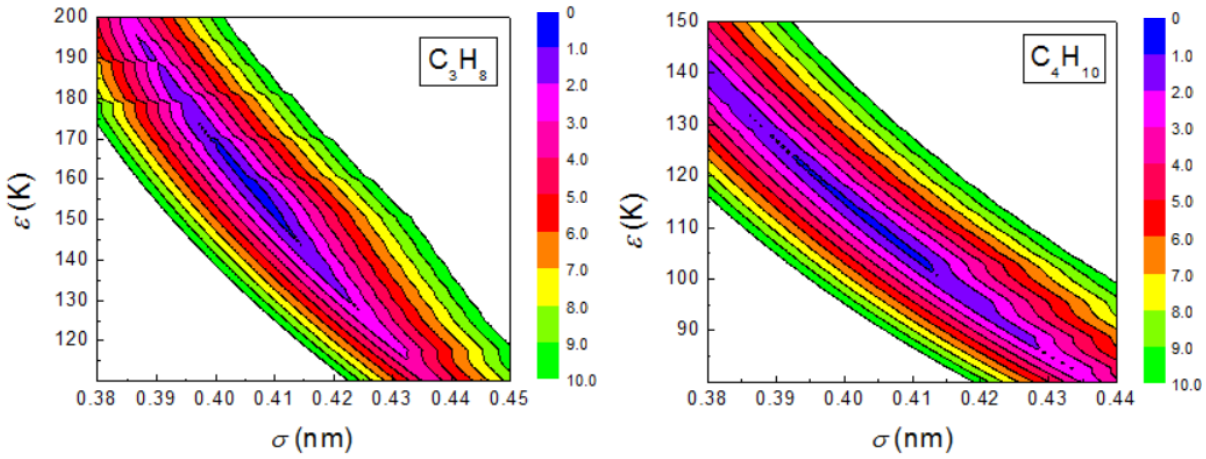

Figure 6: Contour plots of the deviation Δ (see Equation (5)) as a function of ε and σ for propane and *n*-butane. Contours are set to 1.0%, while the band width is 10%. The deviation (Δ) was computed within the experimental range of temperatures for each alkane. Color legends are included on the side of each graph.

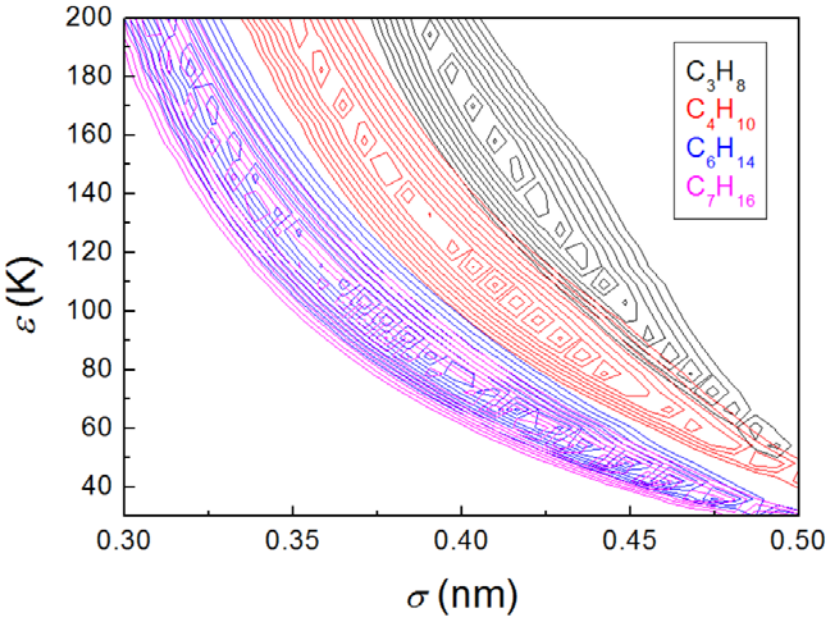

Figure 7: Contour plots of the deviation Δ (see Equation (5)) as a function of ε and σ for propane, *n*-butane, *n*-hexane and *n*-heptane. Contours are set to 1%, while the band width is 10% for all cases.

As it is not possible to mimic the interactions of real *n*-alkane molecules using the described site-site LJ model with a global value of the parameters ε and σ, we take a different approach and examine if there is a trend, as a function of number of segments, that could be made use of. As there is no unique ε - σ pair for each gas, there are a number of ways of choosing the appropriate values. Here, we take advantage of the overall contour plot, Figure 7, and take an arbitrary cut along $\varepsilon = 140$ K. It crosses all the bands in Figure 7, thus allowing us to choose the optimal σ for each gas that will reproduce the viscosity within a certain accuracy. Other cuts along the horizontal, the vertical or in diagonal direction could have been chosen, leading to similar results as long as the central strip of the bands ($\Delta < 1\%$) is crossed. Nevertheless, not all

choices would give sensible values of ε and σ, and for some of the choices the reduced parameters s^* and T^* would fall outside their calculated range.

Figure 8 shows the absolute value of the deviation Δ as a function of the characteristic length σ obtained for the four *n*-alkanes along the $\varepsilon = 140$ K cut. The minimum in Δ allows for a choice of the optimal value of σ that best fits the experimental viscosity data for each *n*-alkane. We observe that the value of Δ is rather sensitive to the value of σ and that a change of 10% in σ will on average result in a change of 17% in Δ. The optimal values of σ where used to calculate the parameter $k \equiv \sqrt{\varepsilon}/\sigma^2$, see Equation (2), and Figure 9 demonstrates that k varies approximately linearly with the number of carbon atoms (n_c). The fitted values of k are given by $k^{\text{fit}} = A + Bn_c$, where $A = (41.38 \pm 5.10)\ \text{K}^{1/2}/\text{nm}^2$ and $B = (9.64 \pm 1.13)\ \text{K}^{1/2}/\text{nm}^2$.

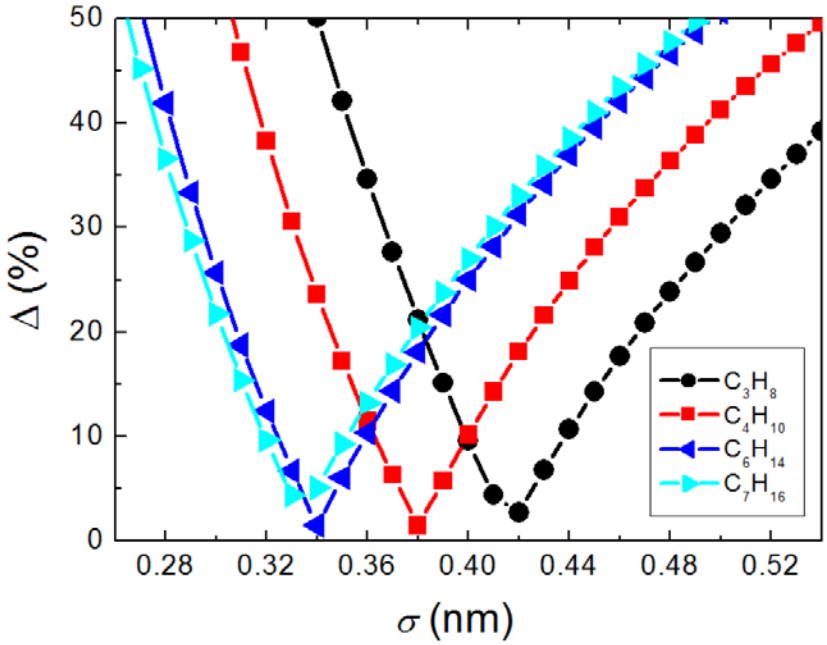

Figure 8: Deviation Δ over the experimental range of temperatures, ΔT_i, as a function of the LJ parameter σ along the $\varepsilon = 140$ K cut.

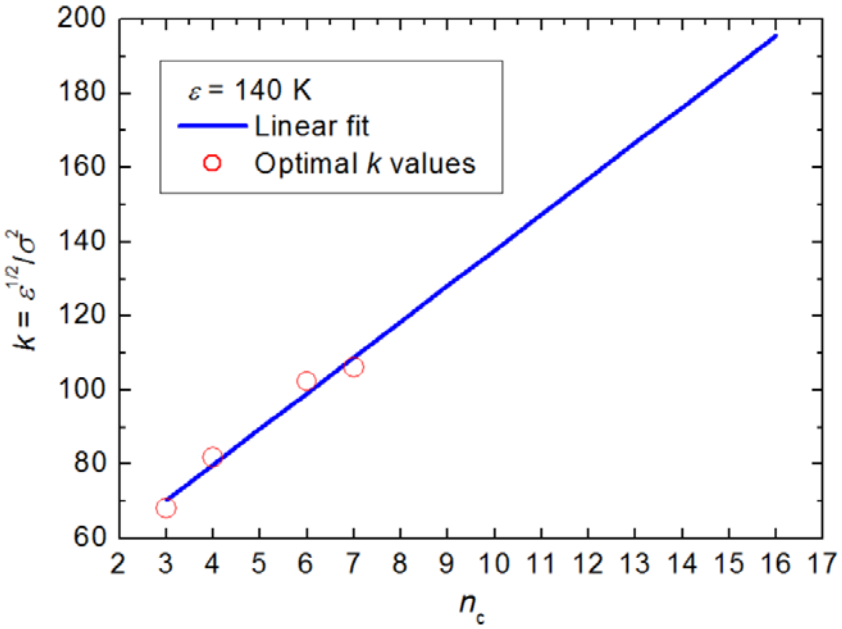

Figure 9: Variation of the parameter $k \equiv \sqrt{\varepsilon}/\sigma^2$ as a function of the number of carbon atoms n_c.

We have used the values of k^{fit} to predict the viscosity of *n*-alkanes for which no correlation is available and compare with the available experimental data. We have made use of seven sets of measurements, consisting of data of Vogel and Holdt [54], Lyusternik and Zhdanov [55,56] and Carmichael *et al.* [57], to perform the comparison. Vogel and Holdt [54] measured the viscosity of *n*-pentane in an oscillating disk viscometer in the temperature range 320–630 K and estimated the accuracy of the zero-density viscosity to be in the range 0.2–0.35%. Lyusternik and Zhdanov [55] performed measurements on *n*-octane, *n*-decane, *n*-dodecane, *n*-tetradecane and *n*-hexadecane in a capillary viscometer in the temperature range 380–723 K with a reported uncertainty of 1.3%. Huber and co-workers [58] used their data as primary when developing correlations for *n*-octane and *n*-decane, but estimated the uncertainty of the correlation to be 5% in the vapour phase. A single viscosity datum for *n*-tridecane at 717.8 K, also measured by Lyusternik and Zhdanov [56], has been obtained from a figure in Ref. [56]. Carmichael and co-workers also measured the viscosity of *n*-decane [57], but using a rotating cylinder viscometer in the temperature range 277–478 K without giving estimates of uncertainty in the vapour phase.

Figure 10 illustrates the relative deviations between the predicted and the experimental viscosity data. We observe in the left panel of the figure that using the fitted k value ($k^{\text{fit}} = 41.383 + 9.639n_c$), we can recover the viscosities of propane, *n*-butane, *n*-hexane and *n*-heptane within ±4%. Although the deviations are much larger than when we use the optimal ε and σ values ($\Delta < 1.6\%$), they are still within reasonable bounds. The right panel of Figure 10 illustrates the deviations observed for fluids that were not used in the fitting procedure. The model predicts the viscosity of *n*-pentane measured by Vogel and Holt [54] with an average absolute deviation (AAD) of 2.1% and a maximum deviation (MaxD) of 2.6%. Although this is outside the claimed uncertainty of the data, it is still within the uncertainty of 4% obtained for propane, *n*-

butane, *n*-hexane and *n*-heptane. The data of Lyusternik and Zhdanov [55,56] for *n*-octane up to and including the data for *n*-tetradecane are recovered with an AAD of 3.9% and a MaxD of 11.8%, with 31 data points out of the total of 36 measured lying within ±5%, which is the uncertainty that Huber *et al.* [58] have assigned to these data. The viscosity data for *n*-hexadecane of Lyusternik and Zhdanov [55] are systematically underpredicted by the current model by 11–25%. However, the three experimental values at the highest temperatures are on average 7–9% higher than the recommended values for *n*-hexadecane given by the same authors in tabular form [55]. If the tabulated values are assumed to be correct, the viscosity data for *n*-hexadecane of Lyusternik and Zhdanov [55] are systematically underpredicted by the current model by only 8–16%. The *n*-decane viscosity data of Carmichael and co-workers was predicted with an AAD of 1.7% and a MaxD of 7.1%. Overall, the proposed k^{fit} model with $\varepsilon = 140$ K is capable of predicting the viscosity in the zero-density limit for propane to *n*-heptane with an uncertainty of 4.5% in the temperature range 293–633 K. For *n*-octane up to *n*-tetradecane, where k^{fit} was extrapolated, the uncertainty is about 12%, while the data for *n*-hexadecane are systematically underpredicted. It is worth noting that the use of an effective spherical LJ 12-6 potential within the model reported previously [29] also systematically underpredicts the measured viscosity of hexadecane, but with a MaxD of only 10%. More importantly, it predicts the tabulated recommended data of Lyusternik and Zhdanov [55] within 2.2%.

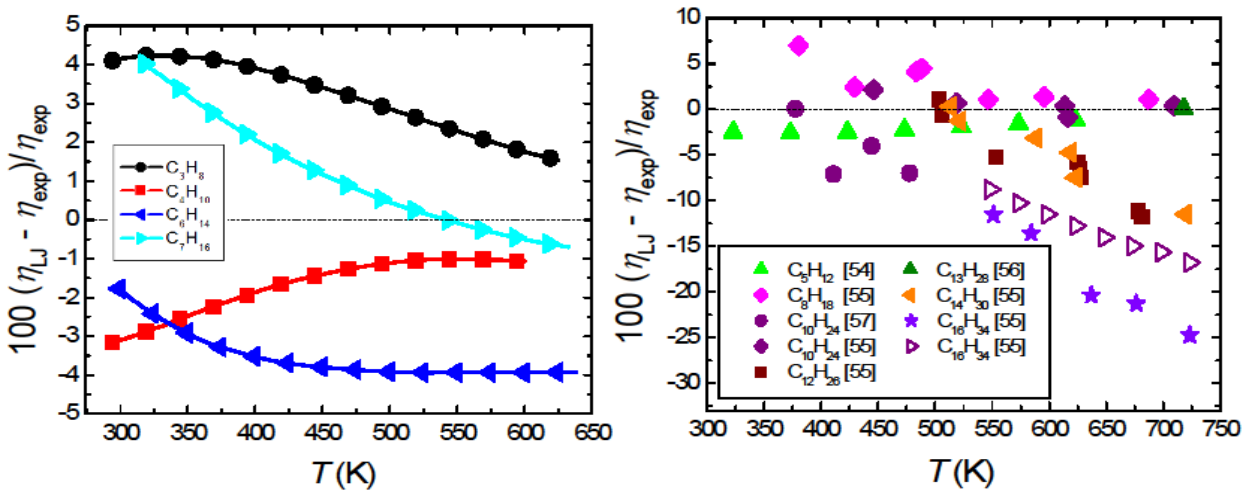

Figure 10: In the left panel, the relative deviations between the calculated viscosity, η_{LJ}, and the experimentally correlated one, η_{exp}, are reported for *n*-alkanes used in developing the correlation for k. In the right panel, the deviations with respect to experimental measurements for other alkanes are reported.
The symbol (▷) in the right panel denotes the relative deviations between the calculated viscosity, η_{LJ}, and the recommended values for the viscosity of *n*-hexadecane [55].

As discussed previously, the choice of $\varepsilon = 140\ \mathrm{K}$ is not the only viable one. A number of other possibilities were examined, including other constant values of ε, constant values of σ and variation of both ε and σ with the number of carbon atoms. We also examined a number of other, less physical models, where $n_\mathrm{s} \neq n_\mathrm{c} - 1$. The overall predictive power of the alternative models was at best similar and in many cases worse than that of the model reported here. Furthermore, for a number of cases it was not possible to obtain a smooth variation in the parameter k, thus limiting the use of the model in the predictive mode.

4. Summary and Conclusions

The shear viscosity in the dilute gas limit has been calculated using the classical trajectory method for a number of *n*-alkanes ranging from propane to *n*-hexadecane. The *n*-alkane molecules were represented as rigid linear chains made up of $n_c - 1$ spherical segments, where n_c is the number of carbon atoms. The chains interact with each other through a Lennard-Jones 12-6 site-site potential, with the sites located at the center of each segment. The distance between two neighbouring sites in a chain was chosen so that the moments of inertia of the rigid chains are equivalent to those of the real *n*-alkane molecules. The reported results show that the viscosity decreases for a given site-site separation with increasing number of segments and decreases, less rapidly, with increasing site-site separation for a given number of segments.

The energy and length scaling parameters, ε and σ, of the site-site LJ 12-6 potential were obtained by fitting to experimental viscosity data of a selected number of *n*-alkanes. For this purpose, we used state-of-the-art viscosity correlations for propane, *n*-butane, *n*-hexane and *n*-heptane that have well-defined uncertainty limits. The results demonstrate that the site-site Lennard-Jones 12-6 potential, when used with the proposed rigid-chain model, can fit the viscosity data of the four n-alkanes, but not within their claimed uncertainty limits. Nevertheless, the model is sufficiently realistic to represent the viscosity of n-alkanes in the dilute gas limit within 1.6%. As expected, the results confirm that for each alkane there is no unique pair of ε and σ values that can fit the viscosity data; rather, there exist a number of possible combinations of the two parameters. Furthermore, it is also clear that there is no single set of ε and σ values that can reproduce the viscosity of all four gases with acceptable accuracy. This indicates that a global LJ site-site potential is not sufficiently flexible to be transferable from one *n*-alkane molecule to another, in order to characterize the effective interactions relevant to viscosity. In other words, the change of the potential when increasing the number of segments in the chain does not mimic the change of the potential when going from one *n*-alkane molecule to another. It is possible that a site-site potential that is more flexible than the LJ 12-6 potential can better address the change in anisotropy of real *n*-alkanes or that non-rigid chains in conjunction with a LJ site-site potential can provide a more realistic description

As the energy and length scaling parameters are not transferrable, a trend among *n*-alkane LJ 12-6 scaling parameters was explored that allows for the prediction of the viscosities of *n*-alkanes for which there is a lack of experimental viscosity data. Due to the non-uniqueness of ε and σ for each alkane, there exist a plethora of possibilities of choosing the appropriate values. Moreover, as the scaling parameters are effective, it is difficult to use sensible physical constraints to differentiate between them. We opted for constraining the value of the energy scaling parameter to $\varepsilon = 140\ \mathrm{K}$. Under these circumstances, the parameter k, defined as $k \equiv \sqrt{\varepsilon}/\sigma^2$, exhibits a near-linear behavior with increasing number of segments. The resulting model is capable of predicting the viscosity in the zero-density limit for propane to *n*-heptane

with an uncertainty of 4.5% in the temperature range 293–633 K. For *n*-octane up to *n*-tetradecane, where the parameter k was extrapolated, the uncertainty is about 12%, while the experimental data for *n*-hexadecane are systematically underpredicted by up to 25%. However, the uncertainty of these data might be higher than expected. Hence, the two questions that were posed as part of this research, (i) can the choice of the length and energy scaling parameters for the site-site potentials be made such as to compensate for the deficiencies of the current model and (ii) will this produce a more accurate way of calculating the viscosity than was achieved by means of an effective spherical LJ 12-6 potential, have to be answered negatively. The current results indicate that the effective site-site LJ 12-6 potentials with scaling parameters obtained from k^{fit} are not suitable for predicting the dilute gas viscosities of *n*-alkanes. The effective scaling parameters have to be obtained by fitting to the experimental viscosity data for each *n*-alkane and are not transferable to other species. Surprisingly, the use of an effective spherical LJ 12-6 potential with extrapolated scaling parameters leads to a better description of the viscosity of *n*-alkanes [29] than the present, more sophisticated model.

Acknowledgements

The authors would like to thank Dr. Nicolas Riesco for the initial analysis of the classical trajectory results.

Disclosure statement

No potential conflict of interest is reported by the authors.

Funding

R.H. gratefully acknowledges financial support by the Deutsche Forschungsgemeinschaft (DFG) through Grant No. HE 6155/2-1. JCCP and VV acknowledge financial support by the Imperial College Trust.

References

[1] F.R.W. McCourt, J.J.M. Beenakker, W.E. Köhler, and I. Kuščer, *Nonequilibrium Phenomena in Polyatomic Gases, vol. I: Dilute Gases* (Clarendon Press, Oxford, 1990).

[2] R. Hellmann, Mol. Phys. **111**, 387 (2013).

[3] E.L. Heck and A.S. Dickinson, Physica A **217**, 107 (1995).

[4] S. Bock, E. Bich, E. Vogel, A.S. Dickinson, and V. Vesovic, J. Chem. Phys. **117**, 2151 (2002).

[5] R. Hellmann, E. Bich, E. Vogel, A.S. Dickinson, and V. Vesovic, J. Chem. Phys. **129**, 064302 (2008).

[6] R. Hellmann, E. Bich, E. Vogel, A.S. Dickinson, and V. Vesovic, J. Chem. Phys. **131**, 014303 (2009).

[7] R. Hellmann, E. Bich, E. Vogel, and V. Vesovic, Phys. Chem. Chem. Phys. **13**, 13749 (2011).

[8] R. Hellmann, E. Bich, and V. Vesovic, J. Chem. Phys. **141**, 224301 (2014).

[9] R. Hellmann, E. Bich, and V. Vesovic, J. Chem. Thermodyn. (2016), submitted.

[10] R. Hellmann, N. Riesco, and V. Vesovic, J. Chem. Phys. **138**, 084309 (2013).

[11] G. Galliéro, C. Boned, and A. Baylaucq, Ind. Eng. Chem. Res. **44**, 6963 (2005).

[12] G. Galliéro and C. Boned, Phys. Rev. E **79**, 021201 (2009).

[13] S. Delage Santacreu, G. Galliéro, M. Odunlami, and C. Boned, J. Chem. Phys. **137**, 204306 (2012).

[14] H. Hoang and G. Galliero, J. Phys.: Condens. Matter **25**, 485001 (2013).

[15] G. Galliéro, Chem. Eng. Res. Design **92**, 3031 (2014).

[16] T.K. Patra, A. Hens, and J.K. Singh, J. Chem. Phys. **137**, 084701 (2012).

[17] T. Goel, C. Nath Patra, T. Mukherjee, and C. Chakravarty, J. Chem. Phys. **129**, 164904 (2008).

[18] X.-G. Zhang and Y.-X. Yu, Fluid Phase Equilib. **295**, 237 (2010).

[19] Y.M. Muñoz-Muñoz, G. Guevara-Carrion, M. Llano-Restrepo, and J. Vrabec, Fluid Phase Equilib. **404**, 150 (2015).

[20] G.A. Fernández , J. Vrabec, and H. Hasse, Mol. Simul. **31**, 787 (2005).

[21] V.G. Baidakov, S.P. Protsenko, and Z.R. Kozlova, Chem. Phys. Lett. **517**, 166 (2011).

[22] A. Ahmed and R.J. Sadus, AIChE J. **57**, 250 (2011).

[23] S.H. Lee, Bull. Korean Chem. Soc. **29**, 641 (2008).

[24] S. Viscardy, J. Servantie, and P. Gaspard, J. Chem. Phys. **126,** 184512 (2007).

[25] K.M. Dyer, B.M. Pettitt, and G. Stell, J. Chem. Phys. **126**, 034502 (2007).

[26] L.V. Woodcock, AIChE J. **52**, 438 (2006).

[27] K. Meier, A. Laesecke, and S. Kabelac, J. Chem. Phys. **121**, 3671 (2004).

[28] G.A. Fernández, J. Vrabec, and H. Hasse, Fluid Phase Equilib. **221**, 157 (2004).

[29] N. Riesco and V. Vesovic, Fluid Phase Equilib. (2016), submitted.

[30] M.J. Assael, A.R.H. Goodwin, V. Vesovic, and W.A. Wakeham, editors, *Experimental Thermodynamics Volume IX: Advances in Transport Properties of Fluids* (The Royal Society of Chemistry, London, 2014).

[31] G.C. Maitland, M. Mustafa, and W.A. Wakeham, J. Chem. Soc., Faraday Trans. **79**, 1425 (1983).

[32] E.L. Heck and A.S. Dickinson, Comput. Phys. Commun. **95**, 190 (1996).

[33] S.L. Tait, Z. Dohnálek, C.T. Campbell, and B.D. Kay, J. Chem. Phys. **122**, 164708 (2005).

[34] M.E. Wieser, *Atomic weights of the elements 2005*, IUPAC Technical Report, Pure Appl. Chem. **78**, 2051 (2006).

[35] W.M. Haynes, editor-in-chief, *CRC Handbook of Chemistry and Physics*., 96th ed. (CRC, Boca Raton, 2015).

[36] J. Millat, J.H. Dymond, and C.A. Nieto de Castro, editors, *Transport Properties of Fluids: Their Correlation, Prediction and Estimation* (Cambridge University Press, Cambridge, 1996).

[37] E. Vogel, C. Küchenmeister, E. Bich, and A. Laesecke, J. Phys. Chem. Ref. Data **27**, 947 (1998).

[38] E. Vogel, C. Küchenmeister, and E. Bich, High Temp. – High Press. **31**, 173 (1999).

[39] E.K. Michailidou, M.J. Assael, M.L. Huber, and R.A. Perkins, J. Phys. Chem. Ref. Data. **42**, 033104 (2013).

[40] E.K. Michailidou, M.J. Assael, M.L. Huber, I.M. Abdulagatov, and R.A. Perkins, J. Phys. Chem. Ref. Data. **43**, 023103 (2014).

[41] S. Chapman and T.G. Cowling, *The Mathematical Theory of Non-uniform Gases*, 3rd ed. (Cambridge University Press, 1970).

[42] J.O. Hirschfelder, C.F. Curtiss, and R.B. Bird, *Molecular Theory of Gases and Liquids* (Wiley, New Jersey, 1954).

[43] T. -S. Ho and H. Rabitz, J. Chem. Phys. **104**, 2584 (1996).

[44] J.C. Castro-Palacio, T. Nagy, R. J. Bemish, and M. Meuwly, J. Chem. Phys. **141**, 164319 (2014).

[45] J.C. Castro-Palacio, R. J. Bemish, and M. Meuwly, J. Chem. Phys. **142**, 091104 (2015).

[46] G.N.I. Clark, A.J. Haslam, A. Galindo, and G. Jackson, Mol. Phys. **104,** 3561 (2006).

[47] D. Reichenberg, *DCS Report 11* (National Physics Laboratory, Tedington UK, 1971).

[48] G. Mie, Ann. Phys. (Leipzig) **11**, 657 (1903).

[49] C. Avendaño, T. Lafitte, A. Galindo, C.S. Adjiman, G. Jackson, and E.A. Müller, J. Phys. Chem. B **115**, 11154 (2011).

[50] T. Lafitte, C. Avendaño, V. Papaioannou, A. Galindo, C.S. Adjiman, G. Jackson, and E.A. Müller, Mol. Phys. **110**, 1189 (2012).

[51] C. Avendaño, T. Lafitte, A. Galindo, C.S. Adjiman, E.A. Müller, and G. Jackson, J. Phys. Chem. B **117**, 2717 (2013).

[52] J. J. Potoff and D. A. Bernard-Brunel, J. Phys. Chem. B **113,** 14725 (2009).

[53] A. Hemmen, A. Z. Panagiotopoulos, and J.Gross, J. Phys. Chem. B **119,** 7087 (2015).

[54] E. Vogel and B. Holdt, High Temp. – High Press. **23**, 473 (1991).

[55] V.E. Lyusternik and A.G. Zhdanov, Teplofiz. Svoistva Veshchestv Mater. **7**, 95 (1973).

[56] V.E. Lyusternik and A.G. Zhdanov, Russ. J. Phys. Chem. **45**, 113 (1971).

[57] L.T. Carmichael, V.M. Berry, and B.H. Sage, J. Chem. Eng. Data **14**, 27 (1969).

[58] M.L. Huber, A. Laesecke, and H.W. Xiang, Fluid Phase Equilib. **224**, 263 (2004).

Table 1: Results for the site-site distance, s, and the length of the chain, l, for the *n*-alkanes studied in this work.

***n*-alkane**	$\boldsymbol{s}$ **(nm)**	$\boldsymbol{l}$ **(nm)**
C_3H_8	0.2302	0.4604
C_4H_{10}	0.1853	0.5558
C_5H_{12}	0.1675	0.6700
C_6H_{14}	0.1580	0.7898
C_7H_{16}	0.1520	0.9119
C_8H_{18}	0.1479	1.0356
C_9H_{20}	0.1447	1.1576
$C_{10}H_{22}$	0.1426	1.2838
$C_{12}H_{26}$	0.1410	1.5511
$C_{13}H_{28}$	0.1400	1.6800
$C_{14}H_{30}$	0.1392	1.8090
$C_{16}H_{34}$	0.1378	2.0672

Table 2: Experimental viscosity data used in this work.

***n*-alkane**	**Authors**	**Temperature range, ΔT_i (K)**	**Claimed uncertainty (%)**
C_3H_8	Vogel *et al.* [37]	293–625	<0.4
C_4H_{10}	Vogel *et al.* [38]	293–600	<0.4
C_6H_{14}	Michailidou *et al.* [39]	298–638	<0.3
C_7H_{16}	Michailidou *et al.* [40]	317–633	<0.3

Figure Captions:

Figure 1: Schematic representation of *n*-pentane by a rigid linear chain of four spherical segments. The blue circles represent the carbon atoms, while the red open circles represent segments.

Figure 2: Reduced viscosity, η^*_{LJ}, of rigid LJ chains for $s^* = 0.25$ as a function of the reduced temperature T^* (left panel) and the number of segments per chain n_{s} (right panel).

Figure 3: Reduced viscosity, η^*_{LJ}, as a function of reduced site-site distance, s^*, for $T^* = 2,\ 4, 10$ and 50. The different curves represent the different number of segments: (—■—), $n_{\mathrm{s}} = 2$; (—●—), $n_{\mathrm{s}} = 3$; (—▲—), $n_{\mathrm{s}} = 4$; (—▼—), $n_{\mathrm{s}} = 6$; (—◆—), $n_{\mathrm{s}} = 8$; (—◀—), $n_{\mathrm{s}} = 12$; (—▶—), $n_{\mathrm{s}} = 16$.

Figure 4: Second-order viscosity correction factor $f_\eta^{(2)}$ of rigid Lennard-Jones chains as a function of the reduced temperature T^* for $s^* = 0.25, 0.333, 0.60$ and 1.0. The different curves represent the different number of segments: (—■—), $n_{\mathrm{s}} = 2$; (—●—), $n_{\mathrm{s}} = 3$; (—▲—), $n_{\mathrm{s}} = 4$; (—▼—), $n_{\mathrm{s}} = 6$; (—◆—), $n_{\mathrm{s}} = 8$; (—◀—), $n_{\mathrm{s}} = 12$; (—▶—), $n_{\mathrm{s}} = 16$.

Figure 5: Relative deviations between the calculated viscosity, η_{LJ}, and the experimental viscosity, η_{exp}. The solid lines represent the RKHS interpolation.

Figure 6: Contour plots of the deviation Δ (see Equation (5)) as a function of ε and σ for propane and *n*-butane. Contours are set to 1.0%, while the band width is 10%. The deviation (Δ) was computed within the experimental range of temperatures for each alkane. Color legends are included on the side of each graph.

Figure 7: Contour plots of the deviation Δ (see Equation (5)) as a function of ε and σ for propane, *n*-butane, *n*-hexane and *n*-heptane. Contours are set to 1%, while the band width is 10% for all cases.

Figure 8: Deviation Δ over the experimental range of temperatures, ΔT_i, as a function of the LJ parameter σ along the $\varepsilon = 140$ K cut.

Figure 9: Variation of the parameter $k \equiv \sqrt{\varepsilon}/\sigma^2$ as a function of the number of carbon atoms n_{c}.

Figure 10: In the left panel, the relative deviations between the calculated viscosity, η_{LJ}, and the experimentally correlated one, η_{exp}, are reported for *n*-alkanes used in developing the correlation for k. In the right panel, the deviations with respect to experimental measurements for other alkanes are reported.
The symbol (▷) in the right panel denotes the relative deviations between the calculated viscosity, η_{LJ}, and the recommended values for the viscosity of *n*-hexadecane [55].